

Absolute cross section measurements for electron impact ionization of Ar^{7+}

S Rachafi†, D S Belić‡, M Duponchelle, J Jureta§, M Zambra, Zhang Hui and P Defrance

Université Catholique de Louvain, Département de Physique, Laboratoire des Collisions Atomiques, Chemin du Cyclotron 2, B-1348 Louvain-la-Neuve, Belgium

Received 20 July 1990, in final form 27 September 1990

Abstract. The first absolute cross section measurements for single and double electron impact ionization of sodium-like Ar^{7+} are reported. The animated crossed beams method has been employed in the energy range from threshold to 3000 eV. The measured cross sections for single ionization are higher than the theoretical and semi-empirical predictions by about 20–50%. This discrepancy has been associated with the contribution of the indirect ionization processes. The double ionization cross section is only 1% of the single one.

1. Introduction

Electron impact ionization of ions plays an important role in astrophysical and laboratory plasmas. The basic ionization process has long been studied, but a fully satisfying description of the problem remains elusive. Particular difficulties are associated with the three-body nature of the problem and the fact that a number of indirect complex mechanisms often contribute to the ionization cross section which require detailed knowledge of atomic structure, resonance configuration mixing, coupling to the continuum, etc. Total ionization cross section measurements are needed to check theoretical approaches, to judge the approximations required to perform calculations and to provide valuable information about the various processes involved.

Studies of ionization along isoelectronic sequences provide some generalization of aspects associated with atomic structure. The Na-like ions are of particular interest because the single electron in the outer shell makes the problem somewhat simpler, while the relatively large number of electrons in the next lower shell provides an amplification to any contribution by inner-shell processes. For the direct ionization of sodium-like ions and for higher charge states the cross section is dominated by inner-shell ionization of the $2p^6$ subshell (Younger 1981). Excitation of an inner-shell electron can populate levels of the ions which are higher in energy than the $3s$ ionization potential. Decay of such resonances usually proceeds rapidly via autoionization so that the excitation event contributes to the ionization cross section. It was demonstrated by Crandall *et al* (1982), Griffin *et al* (1982) and by Gregory *et al* (1987) that the

† Present address: Université Chouaib Doukkali, Faculté des Sciences, BP 20, El Jadida, Morocco.

‡ Present address: Faculty of Physics, PO Box 550, 11000 Beograd, Yugoslavia.

§ Present address: Institute of Physics, PO Box 57, 11000 Beograd, Yugoslavia.

relative importance of excitation autoionization (EA) increases along the Na isoelectronic sequence, and even dominates over the direct ionization for Fe^{15+} .

Another significant contribution to electron-impact ionization could be from the temporary capture of the incident electron with simultaneous excitation of an inner-shell electron. Such resonances decay with sequential emission of two electrons. This process of resonant-excitation double autoionization (REDA) is proposed by LaGattuta and Hahn (1981) and calculated for Fe^{15+} ionization. Another possibility is a resonant-excitation auto-double-ionization (READI) process, introduced by Henry and Msezane (1982), where the incident electron is again captured temporarily with simultaneous excitation of an inner-shell electron, followed by the resonance decays with simultaneous emission of the two electrons, since both electrons could be screened from the target core. This process cannot be separated from REDA in the current experiments, but its evidence is visible below the $2p^53s$ threshold, where REDA cannot contribute. However, there is no experimental evidence for REDA or READI for Na-like ions, yet. A careful experiment has been performed by Gregory *et al* (1987), but the predicted, significant enhancement of Fe^{15+} cross section due to REDA (or READI) was not observed.

Electron impact ionization of the sodium isoelectronic sequence has been extensively studied only for the first few members of the sequence and for Fe^{15+} . Absolute cross section measurements have been performed by Crandall *et al* (1982) for Mg^+ , Al^{2+} and Si^{3+} and by Gregory *et al* (1987) for Fe^{15+} in a crossed beam experiment. Donets and Ovsyannikov (1977) have deduced ionization cross sections for some highly charged ions, including Ar^{7+} , from the ion charge state distribution in an EBIT ion source. Numerical predictions have been made from theory for both direct and indirect processes by Griffin *et al* (1982), LaGattuta and Hahn (1981), Henry and Msezane (1982) and Younger (1981).

The only theoretical result on Ar^{7+} ionization is a distorted-wave Born exchange (DWBE) approximation, performed by Younger (1981). There are no direct cross section measurements of the ionization cross section. The reason for this could be due to the difficulties in preparing a pure ion beam. It is shown by Howald *et al* (1986) that a significant part of Na-like ions, extracted from an electron cyclotron resonance (ECR) ion source, are in the doublet and quartet levels of $2p^53s3p$ configuration, which are metastable. Owing to the mean lifetime of the order of $1\text{--}10\ \mu\text{s}$, such ions produced a large autoionizing background which prevents accurate cross section measurements (as for S^{5+} , Cl^{6+} , Ar^{7+}).

In this paper we report and discuss the first direct cross section measurements of Ar^{7+} for single and double ionization.

2. Method and apparatus

Our measurements have been performed using an apparatus specially designed to study the ionization of highly charged ions by electron impact. The animated crossed beams method (Brouillard and Defrance 1983) has been employed. The experimental set-up is schematically shown in figure 1.

The ion beam is extracted from an ECR ion source (not shown on the figure), which is capable of producing beams of ions in charge states as high as $q = 15$ for argon (Bol *et al* 1987). The usual acceleration voltage of the ions is of the order of a few keV. Extracted ions are focused by use of an electrostatic and a magnetic lens system, before entering the Wien filter (1) for mass and charge analysis. After passing through a pair

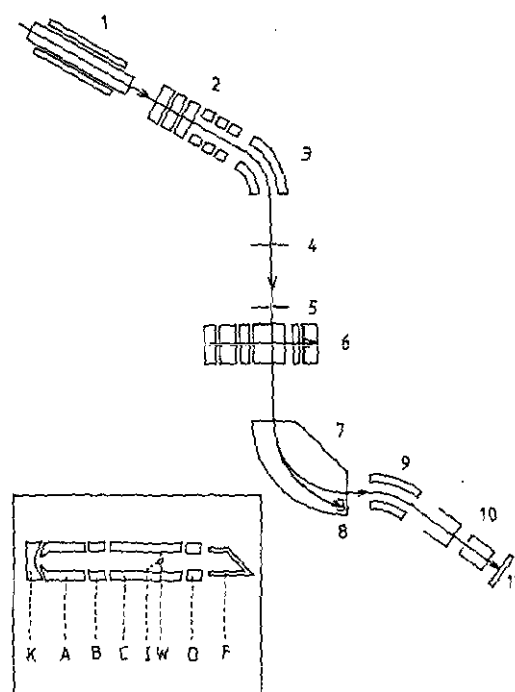


Figure 1. Schematic diagram of the apparatus: 1, Wien filter; 2, electrostatic lenses; 3, electrostatic deflector; 4, 5, diaphragms; 6, electron gun; 7, magnetic analyser; 8, movable Faraday cup; 9, electrostatic deflector; 10, moving slit and Faraday cup; 11, detector. The inset shows a schematic of the electron gun: K, cathode; A, anode; B, focusing and deflection electrodes; C, grounded electrodes; I, ion beam; W, two wires parallel to the ion beam; D, suppressors; F, Faraday cup.

of vertical and horizontal plane einzel lenses (2) the beam is further purified by a 60° electrostatic deflector (3) and collimated by a set of apertures (4, 5) into the collision region. The electron gun (6) is the same as used in previous experiments (Defrance *et al* 1982). In the subsequent 90° magnetic charge state analyser (7) product ions are deflected along an arc with a fixed radius of curvature of 30 cm to the detection system. A movable Faraday cup (8) is adjusted to collect the primary ion beam. Product ions are directed by an electrostatic deflector (9) to the channelplate (11) detection system. A movable device (10) can be introduced into the beam in order to measure the absolute detector efficiency (Brouillard *et al* 1983).

The electron gun is schematically shown on the inset in figure 1. A ribbon-shaped electron beam is extracted from a Pierce-type cathode (K)-anode (A) configuration. The pair of plates (B) acts simultaneously as a lens, and as a beam deflector in the electron beam sweeping mode of the animated crossed beams technique. The electron beam crosses the ion beam (I) at right angle inside the grounded electrode (C). The electrons are collected in a Faraday cup (F). Suppression plates (D) provide total beam collection and prevent secondary electrons from interacting with the ion beam.

In the animated crossed beams method, the electron beam is swept across the ion beam in a linear seesaw motion at constant velocity u which is measured by two thin wires (W) located on both sides of the ion beam symmetrically, perpendicular to the electron beam trajectory.

3. Cross section measurements

The electron impact ionization cross section is related to the measured quantities in the following way (Brouillard and DeFrance 1983):

$$\sigma = \frac{v_e v_i}{\sqrt{v_e^2 + v_i^2}} \frac{uK}{(I_i/qe)(I_e/e)}. \quad (1)$$

Here, u is the scanning velocity, K is the total number of events produced during one passage of electrons across the ion beam, v_e and v_i , I_e and I_i , e and qe are the velocities, currents and charges of the electrons and ions, respectively. In order to achieve good precision, careful measurements are needed for all of the parameters in equation (1).

The electron energy is corrected for contact potential and the kinetic energy of ions is taken into account to obtain the absolute collision energy. The maximum electron energy is 3 keV. In some previous experiments, electron energy distribution (full width at half maximum (FWHM)) is estimated to be less than 1.7 eV.

The scanning velocity u of the electron beam across the ions is determined by measuring the time difference t between successive crossings of the electron beam over the wires (W), for a given amplitude V_1 of the sweeping AC voltage. During the measurements, this amplitude is reduced to a lower value V_2 , so that the electron beam does not reach the wires. This procedure eliminates the production of secondary electrons by the wires. The scanning velocity is then given by the ratio:

$$u = dV_2/tV_1. \quad (2)$$

Here $d = 7.9$ mm is the distance between the wires.

The primary ion beam intensity is measured by the Faraday cup (8) located inside the magnetic analyser (7). The magnetic field ensures total collection of the ions and prevents secondary emission of electrons or ions, which would significantly affect the measurements. The primary ion current is integrated over the measurement time in order to eliminate errors due to the beam fluctuations. All apertures and slits, between the collision region and both primary and product ion detectors, are precisely made to ensure essentially total ion transmission. The total detection efficiency γ is determined by the controlled beam attenuation method (Brouillard *et al* 1983).

The signal delivered by the detector is stored in a multichannel analyser in a multiscaling mode, synchronously with the electron beam sweeping voltage. The usual form of the stored signal consists of two peaks, superimposed on the uniform background level. The peaks are accumulated during the passage of the electron beam upward and downward across the ion beam. The average of the background outside of the peak regions is thus subtracted from the spectra and a net signal for the cross section calculation is obtained.

In this particular experiment some additional difficulties are associated with the signal accumulation because of space charge background modulation and the enormous background count rate level.

Since the ions can be deflected by the space charge of the electron beam (Harrison 1966), the background may be modulated by sweeping the electrons across the ion beam in the animated beams method. This effect is proportional to the electron beam current and varies inversely to the electron velocity (Howald *et al* 1986). It occurs for all the ions in charge states higher than 6 or 7. The consequence is a non-uniform background level in the spectra and usually it gives a spurious signal and therefore larger cross sections. To test for modulation effects in our experiment it is convenient

to plot the cross section as a function of channel number where the peaks are expected. If the plot shows no saturation the signal needs to be corrected for the modulations. This can be done by performing a non-constant fit to the background level for each electron energy. The best fit is observed using a linear function having two parameters. The same procedure is performed also for the data below the 3s threshold ionization energy and as expected zero cross sections are observed within the statistical error bars.

The average signal count rate in this experiment, at the cross section maximum, was of the order $1 \text{ count/nA s}^{-1}$, while the background count rate was of the order of $2000 \text{ counts/nA s}^{-1}$. A number of tests were performed in order to check the origin of the background events.

As already noted, all slits and apertures are dimensioned in order to achieve total ion beam transmission. When we changed the beam focusing parameters we found that only a negligible fraction of background events came from the photons produced when energetic ions hit surfaces. Only a few background events are associated with the x-rays from the ion source. Most of the background was proportional to the Ar^{7+} beam current and it was quasi-independent of the pressure. The count rate of detected Ar^{8+} normalized to the Ar^{7+} current increases only by about 10% when the pressure in the beam transport line and collision chamber was increased from 10^{-9} to 10^{-5} mbar. This increase is due to the stripping of an electron from Ar^{7+} by the residual gas atoms and molecules. The cross section for electron stripping from the ground state Ar^{7+} by H_2 , at the same ion energy, is about $2 \times 10^{-22} \text{ cm}^2$ (Fleischmann *et al* 1972). By contrast, in a separate experiment we have estimated the cross section for stripping to be of the order of $9 \times 10^{-15} \text{ cm}^2$, most likely it is due to the metastable states involved and other higher-order mechanisms such as collision-induced autoionization or capture followed by double autoionization or auto-double-ionization.

The main fraction of the background was independent of residual gas pressure and is also attributed to the presence of metastable ions, having relatively long lifetimes against autoionization, in the ion beam. If such metastable levels autoionize before the post-collision charge state analysis produced ions contribute to the ionization background. It is already shown by Howald *et al* (1986) that the Na-like ions extracted directly from the ECR source (e.g., S^{5+} , Cl^{6+} , Ar^{7+}) produce large autoionizing backgrounds, of the order of 10^3 – 10^4 s^{-1} (particle nA^{-1}). This has been attributed to autoionization of doublet and quartet metastable levels of the $2p^5 3s 3p$ configuration (Harris *et al* 1984). The mechanism proposed for population of metastable levels is ejection of a 2p electron from parent Mg-like $2p^6 3s^3 \text{P}$ metastable levels, which are present in the Mg-like ion beams extracted from the ECR ion source.

In order to check the proposed mechanism for production of metastable ions we measured the ionization background count rate normalized to the Ar^{7+} current as a function of the microwave power injected into the ECR source and therefore argon ion charge state distribution. The result showed that the metastable population depends on the number of Ar^{8+} ions created in the source (and not on Ar^{6+}). We believe that the metastables are produced by capture of an electron by an Ar^{8+} ion with the simultaneous excitation of an inner-shell 2p electron, or most likely by capture of an electron by an Ar^{8+} ion being in the metastable $2p^5 3s^3 \text{P}_{0,2}$ configuration. This configuration has a very long lifetime, $\tau \approx 0.34 \text{ ms}$ (Fielder *et al* 1979), and a large partial capture cross sections in $n=5$ levels, $\sigma_{5p} \approx 2.9 \times 10^{-15} \text{ cm}^2$ and $\sigma_{5d} \approx 3.4 \times 10^{-15} \text{ cm}^2$ (Boudjema *et al* 1988). Resulting $2p^5 3s 5l$ states can rapidly cascade (Bliman *et al* 1989), into doublet and quartet levels of the $2p^5 3s 3l$ configurations which are metastable against autoionization (Harris *et al* 1984). In particular, the $^4\text{D}_{7/2}$ state is predicted to

be very stable against both autoionization and radiative stabilization (Dubau and Cornille 1986). By varying the velocity of the Ar^{7+} beam, we were able to deduce that the mean lifetime of the metastable levels in Ar^{7+} is about $4 \mu\text{s}$.

By reducing the power of the ion source the ratio of signal/background count rate was increased to about 1% during the measurements but several hours of data accumulation were still necessary in order to achieve 10% counting statistics.

Typical working conditions in the present experiment were $I_e = 5 \text{ mA}$, $I_i = 15 \text{ nA}$, $u = 40 \text{ cm s}^{-1}$ and $\gamma = 0.78$. $K = 0.1$ and 0.01 for single and double ionization experiments respectively.

The total systematic uncertainty of the measurements is estimated to be less than 5%. This includes uncertainties due to the determination of the kinematic parameter (0.5%), beam currents (0.5%), detection efficiency (1.7%) and scanning velocity (1.7%). For single ionization data, the statistical uncertainty at the cross section maximum is about 11%, and the total uncertainty obtained in a quadrature sum of systematic and statistical uncertainty is found to be around 12%. The corresponding figure for double ionization is of the order of 50%.

4. Results and discussion

The results of absolute cross section measurements for single ionization of Ar^{7+} with electron energy are listed in table 1. The errors listed in the table represent one standard deviation of the counting statistics, only. The results are shown graphically in figure 2, together with other existing experimental results, theoretical calculations and semi-empirical predictions.

There is only one experimental value of the cross section to be compared with our results at the electron energy of 2500 eV. This point is obtained by Donets and Ovsyannikov (1977) from the charge state distribution analysis in an EBIS ion source. The cross section value agrees with our data within the statistical errors. The cross sections obtained from the semi-empirical formula of Lotz (1968), which include direct 2p and 2s inner-shell contributions, are smaller than our values in a wide energy range by about 20% at the cross section maximum. Comparisons are also made with the distorted-wave Born exchange (DWBE) calculations performed by Younger (1981), who included inner-shell electrons as well. His theoretical cross sections are also smaller than ours over a wide electron energy range by about 25% at the cross section maximum. It is shown, however, by Crandall *et al* (1982) that the DWBE approximation overestimates the measured cross section for the direct ionization of Mg^+ and Al^2 , while the Si^{3+} cross section is well reproduced by the theory below the EA threshold energy.

In order to explain the discrepancy between our results and theory we must consider the contribution to the total effective ionization cross section due to the excitation autoionization. The autoionizing resonances in the ejected electron continuum of Na-like structure have substantial electron excitation cross sections which increase rapidly with Z relative to the direct ionization cross section. For Mg^+ , where almost all the ions in levels above the 3s ionization limit are expected to autoionize, Moores and Nussbaumer (1970) have calculated a 25% increase in the total ionization cross section due to the excitation to the autoionizing states. Griffin *et al* (1982) have estimated this increase to be half of that value, but the contribution measured by Crandall *et al* (1982) was found to be only of the order of a few per cent. For Fe^{15+} ,

Table 1. Absolute cross sections for single ionization of Ar^{7+} . The uncertainties are one standard deviation of counting statistics only.

Electron energy (eV)	Cross section (10^{-18} cm^2)	Uncertainty (10^{-18} cm^2)
98	0.18	0.80
132	0.64	0.38
148	1.18	0.77
198	1.26	0.61
238	1.09	0.32
248	1.29	0.63
263	1.51	0.76
278	1.08	0.79
288	1.32	0.91
298	1.38	0.28
313	1.53	0.77
328	1.66	0.38
388	1.02	0.38
423	1.22	0.56
463	1.16	0.65
473	0.99	0.22
498	1.19	0.21
598	1.63	0.25
698	1.97	0.23
798	2.18	0.24
998	1.76	0.23
1248	2.03	0.30
1498	1.79	0.18
1748	1.68	0.27
1998	1.53	0.18
2248	1.60	0.30
2498	1.71	0.18
2748	1.65	0.19
2998	1.69	0.24

Cowan and Mann (1979) and LaGattuta and Hahn (1981) calculated that the dominant contribution in the total cross section is due to the EA mechanism. This prediction has been confirmed by measurements of Gregory *et al* (1987). There are no calculations of the EA on Ar^{7+} , but from the increasing trend of its relative importance along the sequence one may expect a significant contribution to the total cross section. In order to visualize this contribution we have subtracted the results of Younger (1981) from our experimental data, and the difference is shown in figure 3. We must admit at this point that the error bars are large and therefore any conclusion would be tentative.

There are a large number of autoionizing levels of Ar^{7+} which can contribute to the ionization cross section, in the energy range above 240 eV (Bliman *et al* 1989), some of them with higher probability for autoionization than for radiative stabilization. We believe that most of the indirect cross section is due to the EA process. It is possible also that exotic higher-order mechanisms such as REDA or READI also contribute to Ar^{7+} ionization. Significant enhancement has been predicted by LaGattuta and Hahn (1981) in the Fe^{15+} ionization cross section due to the REDA process. However, this effect has not been observed in a careful experiment performed by Gregory *et al* (1987). A dozen Ar^{7+} levels, which can lead to REDA, are calculated by Hahn (1987) to be in

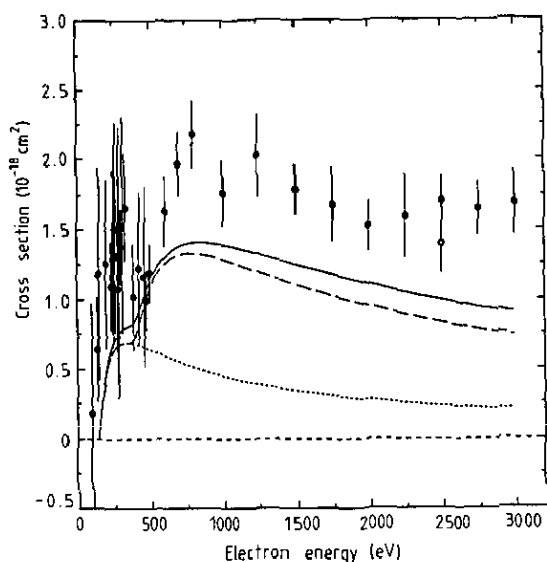


Figure 2. Cross section for electron-impact ionization of Ar^{7+} : \bullet , our results; \circ , Donets and Ovsyannikov (1977); ---, Younger (1981), all subshells, and \cdots , 3s subshell only; — Lotz (1968). The error bars are one standard deviation statistical uncertainties only.

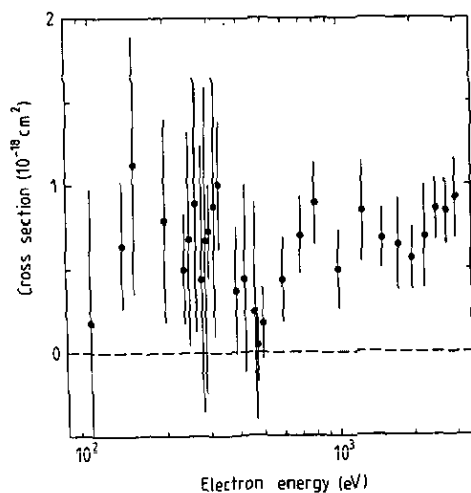


Figure 3. Estimated cross section due to the indirect ionization mechanisms obtained by subtracting the results of Younger (1981) for direct ionization from our experimental data for Ar^{7+} ionization.

the energy region from 247 to 287 eV. These resonances have configurations which are included in previous calculations of REDA in Fe^{15+} . If the branching ratio changes significantly for the same configuration along the isoelectronic sequence, or if the autoionizing lifetimes for Ar^{7+} resonances are short enough to decay before entering the analyzing magnet in our experiment, it might be possible to attribute a fraction of the apparent peak between 240 and 300 eV to the REDA contribution. Of course, this

is only speculation and more careful experiments need to be performed before making any definite conclusion.

The results of absolute cross section measurements for double ionization of Ar^{7+} are listed in table 2 and shown in figure 4. Direct double ionization can be obtained after ejection of electrons belonging to $n=3$ and $n=2$ shells. The thresholds corresponding to the particular electron pairs are estimated from the Hartree-Fock structure calculations by Clementi and Roetti (1974). In addition, a two-step process can contribute to the total cross section; K-shell ionization followed by Auger decay. These threshold energies are listed in table 3 and indicated in figure 4.

Table 2. Absolute cross sections for double ionization of Ar^{7+} . The uncertainties are one standard deviation of counting statistics only.

Electron energy E_e (eV)	Cross section (10^{-20} cm^2)	Uncertainty (10^{-20} cm^2)
550	-0.06	0.78
630	-0.48	0.51
830	0.32	0.64
900	-0.03	0.34
950	0.81	0.54
1000	1.45	0.40
1100	0.74	0.46
1200	0.91	0.59
1500	1.09	0.66
1750	1.36	0.66
2000	1.69	1.60
2250	1.12	0.38
2500	1.46	0.52
2750	1.82	0.74
3000	1.41	0.76

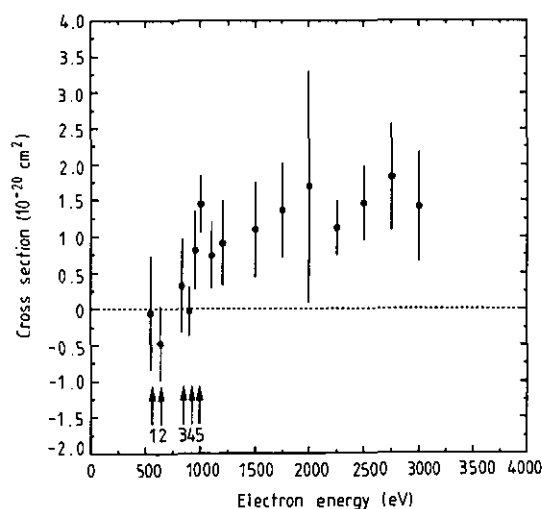


Figure 4. Cross section for electron impact double ionization of Ar^{7+} . The bars are one standard deviation statistical uncertainties only. Arrows indicate the position of ionization thresholds corresponding to different electron pairs (see text).

Table 3. Double ionization thresholds for Ar^{7+} .

Electron shells	Energy (eV)
3s, 2p	566
3s, 2s	641
2p, 2p	846
2p, 2s	921
2s, 2s	996
1s, —	3361

The observed threshold is of the order of 950 eV; i.e., well above the first ionization threshold. This fact indicates that double ionization becomes significant when two electrons are ejected from the same n shell. The indirect double ionization threshold is outside the present energy range. The ratio between double and single ionization is of the order of 1%. Unfortunately, because of the lack of experimental and theoretical results, no further comparison can be made.

5. Summary

We have reported here the first experimental results of absolute cross section measurements for single and double ionization of Na-like Ar^{7+} by electron impact, performed by the animated crossed beams method. For single ionization, comparisons with theoretical predictions indicate that the direct ionization is dominated by the inner-shell process and that a significant contribution of the cross section is due to indirect ionization processes.

Acknowledgments

This work was partially supported by the Fonds National de la Recherche Scientifique and by the Service de la Programmation Scientifique of the Belgian Government. Authors are grateful to the Nuclear Physics Group of the University for using the OCTOPUS ion source for Atomic Collision Physics. The authors are grateful to Y Hahn and to J Dubau and M Cornille for many fruitful discussions, and for providing their energy-level and lifetime calculations to us. One of us (DSB) acknowledges support by NBS through NBS (G)-691-YU.

References

- Bliman S, Suraud M G, Hitz D, Rubensson J E, Nordgren J, Cornille M, Indelicato P and Knystautas E J 1989 *J. Phys. B: At. Mol. Opt. Phys.* **22** 3647
- Bol J L, Chevalier A, Jongen Y, Lacroix M, Mathy F and Ryckewaert G 1986 *Proc. 11th Int. Conf. on Cyclotrons and their Applications (Tokyo)* ed M Sekiguchi, Y Yano and K Hatanaka (Tokyo: Ionic) p 90
- Boudjema M, Benoit-Cattin P, Bordenave-Montesquieu A and Gleizes A 1988 *J. Phys. B: At. Mol. Opt. Phys.* **21** 1603

- Brouillard F, Chantrenne S, Claeys W, Cornet A and Defrance P 1983 *Proc. 13th Int. Conf. on Physics of Electronic and Atomic Collisions (Berlin)* (Amsterdam: North-Holland) Contributed papers p 713
- Brouillard F and Defrance P 1983 *Physica Scripta* **T3** 801
- Clementi E and Roetti C 1974 *At. Data Nucl. Data Tables* **14** 177
- Cowan R D and Mann J B 1979 *Astrophys. J.* **232** 940
- Crandall D H, Phaneuf R A, Falk R A, Belic D S and Dunn G H 1982 *Phys. Rev. A* **25** 143
- Defrance P, Chantrenne S, Brouillard F, Rachafi S, Belic D, Jureta J and Gregory D 1981 *Nucl. Instrum. Methods B* **9** 400
- Defrance P, Claeys W and Brouillard F 1982 *J. Phys. B: At. Mol. Phys.* **15** 3509
- Donets E D and Ovsyannikov V P 1977 *JINR Report* no P7-10780
- Dubau J and Cornille M 1986 Private communication
- Fielder W Jr, Ling-Dan L and Ton-Thaf Dinh 1979 *Phys. Rev. A* **19** 741
- Fleischmann H H, Dehemel R C and Lee S K 1972 *Phys. Rev. A* **5** 1784
- Gregory D C, Wang L J, Meyer F W and Rinn K 1987 *Phys. Rev. A* **35** 3256
- Griffin D C, Bottcher C and Pindzola M S 1982 *Phys. Rev. A* **25** 154
- Hahn Y 1987 Private communication
- Harris S E, Walker D J, Caro R G, Mendelson A J and Cowan R D 1984 *Opt. Lett.* **9** 168
- Harrison M F A 1966 *Br. J. Appl. Phys.* **17** 371
- Henry R J W and Msezane A Z 1982 *Phys. Rev. A* **26** 2545
- Howald A M, Gregory D C, Meyer F W, Phaneuf R A, Müller A, Djuric N and Dunn G H 1986 *Phys. Rev. A* **33** 3779
- LaGattuta K J and Hahn Y 1981 *Phys. Rev. A* **24** 2273
- Lotz W 1968 *Z. Phys.* **216** 241
- Moores D L and Nussbaumer H 1970 *J. Phys. B: At. Mol. Phys.* **3** 161
- Younger S M 1981 *Phys. Rev. A* **24** 1272